



Investigation on post heat treatment parameters of additively manufactured AlSi10Mg parts in terms of time and build direction

Eklemeli imalat ile üretilmiş AlSi10Mg parçalara ardıl ısıl işlem süreleri ve üretim yönü parametrelerinin etkisinin incelenmesi

Remzi Ecmel Ece^{1,*} , Ömer Keleş² , Bekir Sami Yılbaş³ 

¹ Turkish Aerospace Industries Inc., 06980, Ankara, Türkiye

² Gazi University, Mechanical Engineering Department, 06570, Ankara, Türkiye

³ King Fahd University of Petroleum and Minerals, Mechanical Engineering Department, 31261, Dhahran, Saudi Arabia

Abstract

This study reports the combinatorial influence of build direction and different ageing times. The Additively Fabricated (AF) with selective laser melting (SLM) specimens built-in various build directions (0° – 45° - 90°). Accordingly, Solution Heat Treatment (SHT) was applied then quenched in water at room temperature afterward. Subsequently, T4 and T6 ageing procedures were executed. Besides achieving advantageous T6 artificial ageing (AA), specimens were exposed to different time combinations (0.5, 1, 2, 6, 10 h). Although it was observed that the density did not change significantly with heat treatment, it was indicated that the hardness value decreased around 35% with the decrease in time, especially for T6 conditions. The microstructure disparity as a function of the utilized temperature, build direction, and time of the specimens were correlated to hardness values. It was observed that build direction and relative density results have no significant effect on the hardness.

Keywords: AlSi10Mg, SLM, Powder bed fusion, Ageing

1 Introduction

AM is a technique that has been trying to find a place in the industry since the 1980s. It has been on the agenda due to the development of technology and has not been able to find the value it deserves due to technological constraints [1,2]. The key advantage of AM is the capability of manufacturing lightweight, robust and complex shapes owing to layer by layer manufacturing methodology directly from computer-aided design (CAD) data. In the last few decades, interest in this technology has increased due to the fact that AM is one of the core methodologies of industry 4.0 [3,4].

Laser Powder Bed Fusion (LPBF) is one of the most prevalent techniques amongst the available AM processes that gives an opportunity to produce complex parts rapidly [5]. LPBF, also known as SLM or Direct Metal Laser Sintering (DMLS), is great interest. Regarding this technique, build volume is one of the drawbacks. Moreover, surface roughness and cost-effectivity also need to be

Öz

Bu çalışmada, Eklemeli İmalat ile üretilmiş parçaların inşa yönü ve farklı yaşlandırma sürelerinin parça üzerindeki etkileri incelenmiştir. Seçici Lazer Ergitme yöntemi (SLE) ile 0° – 45 – 90° inşa yönlerinde üretilmiş numunelere daha sonra çözeltiye alma ısıl işlemi uygulanmıştır. Takiben oda sıcaklığında su verme işlemine tabii tutulmuştur. Ardından da T4 ve T6 yaşlandırma işlemleri uygulanmıştır T6 yapay yaşlandırma işleminin avantajlarını görebilmek için numunelere farklı sürelerde ısıl işlem uygulanmıştır. Isıl işlemle yoğunluğun önemli ölçüde değişmediği görülmekle birlikte, özellikle T6 koşulları için ısıl işlem süresinin artmasıyla birlikte sertlik değerinin %35 civarında azaldığı belirtilmiştir. Uygulanan sıcaklığın, inşa yönünün ve ısıl işlem sürelerinin bir fonksiyonu olarak mikro yapıdaki düzensizlikler incelenmiş ve sertlik değerleriyle ilişkilendirilmiştir. İnşa yönü ve yoğunluk sonuçlarının sertlik üzerinde önemli bir etkisinin olmadığı görülmüştür.

Anahtar kelimeler: AlSi10Mg, SLM, Toz yataklı füzyon, Yaşlandırma

considered. Furthermore, the mechanical and geometrical quality of built parts highly depends on relative density and surface roughness [6].

Aluminium (Al)-Silicon (Si) alloys have become a highly preferred material in the industry due to their superior properties, such as good strength to weight ratio, high corrosion resistance, cost-effectiveness, and commercial availability [7]. In several publications, thermal post-processing parameters have been discussed [8-11]. Moreover, additively manufactured parts require specific post-processes to achieve good mechanical properties (mainly hardness and tensile strength). In general, specific heat treatments are applied, such as stress relief, low-temperature annealing, and natural/artificial ageing (T4, T6) to minimize residual stresses, achieve fine microstructure, and increase the toughness fatigue as creep properties [12-18]. The increase of mechanical properties at macroscale depends on the amount, distribution, and size of magnesium silicide (Mg₂Si) and Si in solid solution strengthening dislocation hardening and Hall-Petch like strengthening [19-

* Sorumlu yazar / Corresponding author, e-posta / e-mail: ecmelece@gmail.com (R. E. Ece)

Geliş / Received: 20.06.2022 Kabul / Accepted: 01.07.2022 Yayınlanma / Published: 14.10.2022

doi: 10.28948/ngumuh.1133444

21]. In addition, the supersaturation of Si due to rapid cooling affects the cellular eutectic microstructure [21-23].

The presented study aims to observe optimum ageing parameters of the most used variation of Al-Si alloy's (AlSi10Mg) for T4 and T6 treatment conditions for samples fabricated with three different angles from the built plate (0°-45°-90°) regarding the heat treatment time. The microstructure dissimilarities consequential from the executed post treatments were interrelated to mechanical properties in terms of hardness, SEM, and XRD analyses.

2 Materials and methods

In this experimental study, commercially available gas atomized AlSi10Mg powder was used provided from GE Additive. The size distribution is 10 – 45 µm, while the average size is ~30 µm. The chemical composition of the powder is tabulated in Table 1. The powder morphology is spherical and has a fine satellite particle in which most of the sizes are less than 5 µm, as shown in Figure 1.

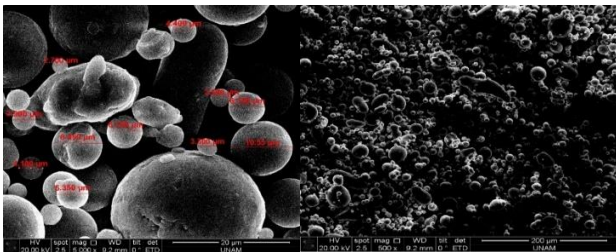


Figure 1. AlSi10Mg powder SEM micrograph showing the powder shapes

A Concept Laser M2 Cusing machine capable of Laser Powder Bed-Fusion was used for specimen fabrication. The system has a Yb-fibre laser with powers up to 400 W and a 60 µm laser spot size. The processing atmosphere is Argon, and Oxygen content was below 0.1 %. Chessboard scanning technique was applied for specimen fabrication which is not especially preferred. However, it is the standard scanning strategy of the Concept Laser System. The bi-directional scanning method has been applied as the laser scanning parameter for the inside of each island [24]. After melting of each islands, laser scans the all periphery of the layer to improve the surface finish. These islands are translated in the x, and y directions 1mm for each following layer and the inner scanning direction of the islands are changed by 90°. Samples were fabricated in three orientations according to build table (Figure 2). The long axis chosen perpendicular to the building table for vertically built samples. (coded below as AF-V; T4-V; T6-V / V:Vertical). According to the build table surface, the transversal direction is manufactured as 45° (coded below as AF-T; T4-T; T6-T / T: Transversal). Horizontally built samples (coded below as AF-H; T4-H;

T6-H / H: Horizontal) are positioned parallel to the fabrication & gas flow direction. The subsequent parameters were used: Laser power (P) 370 W, 1400 mm/s scan speed (Vs), layer thickness (Lt) of the part 25 µm. The hatch distance (Hd) was 112 µm while the energy density was calculated from the Equation 1 below and led to 94.38 J/mm³

$$Ed = P/(Vs \times Hd \times Lt) \quad (1)$$

Note that, as the current study assesses the influence of post-processing rather than the manufacturing parameters. So that the selected parameters were acceptable.

Specimens were first manufactured as cylindrical tensile test specimens with ø10 mm diameters, then cut to novel cylindrical samples with 10 mm heights from the top of each sample for heat treatment trials (Figure 2).

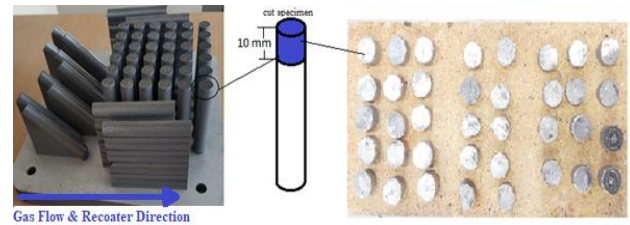


Figure 2. Test specimen manufacturing

According to the composition obtained from the energy-dispersive X-ray spectroscopy (EDS) analysis and thermodynamic calculations from the composition, 520°C must be exceeded to dissolve Mg₂Si. The samples were heated up to 530°C and dwelled for 2 hours for the solution heat treatment process, then quenched into water at room temperature (RT) (22°C) for approximately 30 minutes. Following this procedure, some samples were reserved for natural ageing for 96 hours. The rest were artificially aged at 200°C with different time intervals (0.5, 1, 2, 6, 10 hours) and cooled in the air afterward (Figure 3).

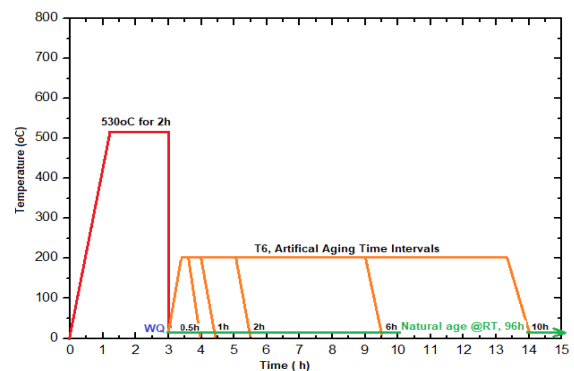


Figure 3. Schematic schedule of the ageing post-process

Table 1. Chemical composition of AlSi10Mg powder

	Al	Si	Fe	Mn	Mg	Ti	Zn	Sn	Cu	Ni	Pb
Bal.		9.6	0.16	<0.01	0.36	<0.01	<0.01	<0.01	<0.01	<0.01	<0.01
%wt		9	Max.	Max.	0.20	Max.	Max.	Max.	Max.	Max.	Max.
		11	0.55	0.45	0.45	0.15	0.10	0.05	0.05	0.05	0.05

3 Results and discussion

3.1 Hardness and relative density vs. heat treatment

HR-15T microhardness measurements were performed with an EMCO-TEST/DuraScan hardness testing device with an applied load of 100gf according to the ASTM - E384 standard with a dwell time of 5 s. At least five measurements were taken from different zones of the etched surface. 100 mL of Keller's etching solution was prepared with a composition of 2.5 mL HNO₃ (nitric acid), 1.5 mL HCl (hydrochloric acid), 1 mL HF (hydrogen fluoride), and 95 mL H₂O (water). Etching was applied before the hardness measurement to determine the non-porous zones and increase the measurements' accuracy. Measurements were averaged and are depicted in Figure 4 with an error margin of 1 %. It is observed that the hardness increases in the range of 10 – 30 % in all directions as a result of T4 and T6 ageing.

Moreover, it was determined that the maximum hardness was reached in the T6 – 2 h samples, among which the highest hardness was achieved in T6 – 2 h samples, which were horizontal. However, lower hardness values were obtained in the T6 ageing process than AF in samples where 0.5 and 1 h were used. After 2 hours, there was an average decrease of 32 % compared to the maximum hardness in heat treatments. Because of the rapid cooling caused by the amount of laser energy corresponding to the unit area and the fact that this occurs quickly and prevents recrystallization and coarsening of the grain structure, higher hardness values were achieved [25-27].

Porosity is an important parameter for the mechanical behaviour of the materials for the parts produced by AM. The formation of porosity changes the bulk density of the material. In this context, density measurements were carried out for the materials produced. Density measurements were carried out in the Mettler-Toledo-XS204 device according to the Archimedes principle. The weight of the samples was measured by device first in the air and then immersing the samples in water. It was observed that the aging process did not have a significant effect on reducing the porosities. Among the AF samples, the lowest density was observed in horizontal samples and the highest density was observed in

vertical samples. Measurements indicates that this situation is due to the relatively low amount of porosity seen in vertical samples. No significant difference was detected in terms of density for the diagonal samples. There is a small amount of irregular increase in density for aging applied samples, unlike the AF samples. Similar results are also stated in some publications in the literature [28-30].

3.2 XRD results

Figures 5(a-c) present XRD spectral patterns of AM-AISI10Mg alloys fabricated in three different directions by the built table (0°, 45°, 90°) of the as-built, natural, and artificially aged conditions. A PANalytical X-Pert-Pro XRD machine was used for the analyses. The values in the graph are normalized to the highest peak of Al (111) such that all the data is presented in the same graph. Rapid cooling causes micro-solidification such that in the Al matrix, a limited quantity of Si peaks was noticed in the as-fabricated alloy, representing that a significant quantity of Silicon particles was supersaturated. The intensity of Si peaks increased after the 2 h SHT process but did not change drastically following Artificial Aging for 6 and 10 h. A small amount of a Mg₂Si phase could be detected at around 58° (220) and 100° (620) for T6 and as fabricated specimens. The crystallographic texture was observed in the XRD patterns of all plots; Al (111) presence the most substantial peak in the pattern, Si (200) revealed comparable intensity to Al (111) in the horizontal and transversal cross-section. On the contrary, Si (200) peaks are much higher than Al (111) peaks. The texture stated from XRD reveals that there is a thermal gradient along with the three directions during the process, which affects the preferential growth of Al along with the (111) orientation. In addition, the Al (200) peak of the vertical samples had a stronger concentration in contrast to horizontal and transversal samples. This slightly different texture in the three directions signifies that the vertical direction's energy density per unit area is higher than in the other directions. Note that similar texture behaviour remained for other directions after natural and artificial heat treatments.

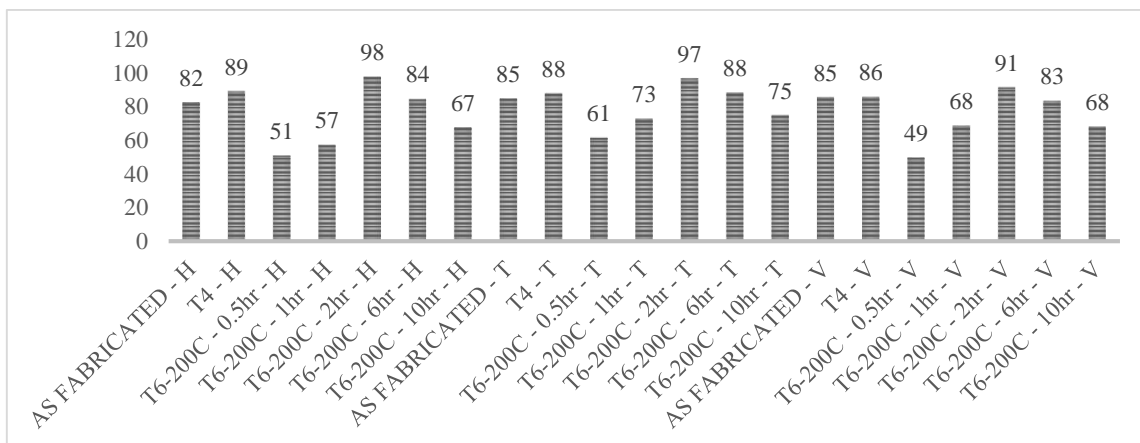


Figure 4. Hardness results of AM-AISI10Mg samples according to the HR-15T hardness measurement method

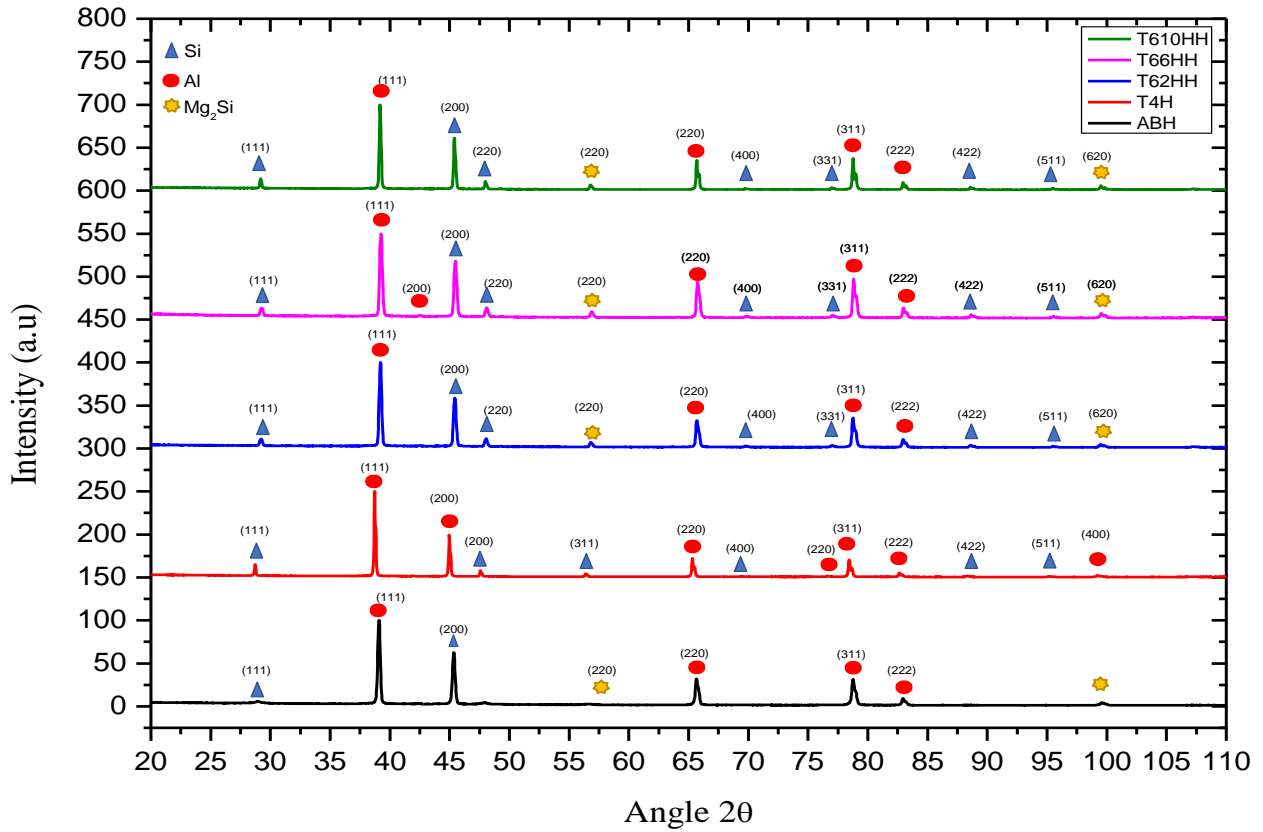


Figure 5a. XRD patterns of horizontal (0°) AM-AlSi10Mg samples AF-As fabricated, T4 naturally and T6 artificially aged samples (2 h, 6 h, 10 h)

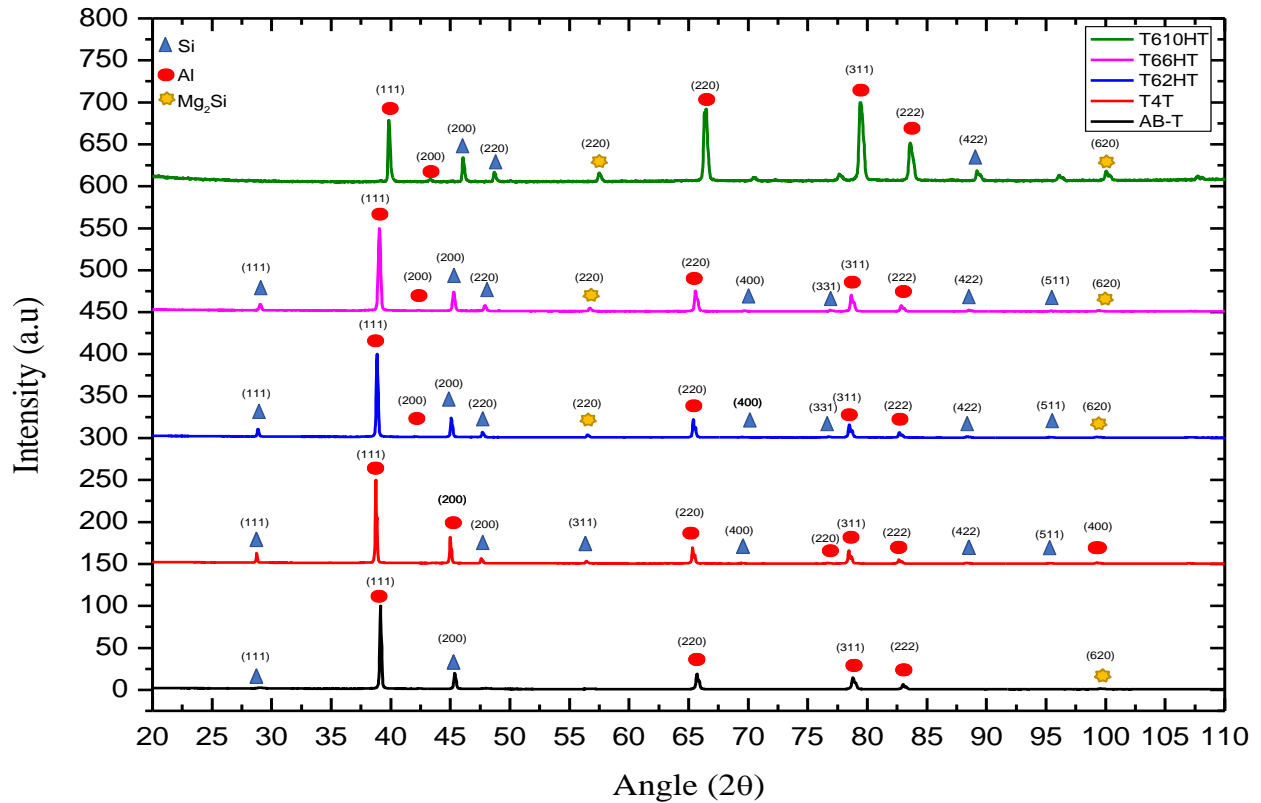


Figure 5b. XRD patterns of transversal (45°) AM-AlSi10Mg samples AF-As fabricated, T4 naturally and T6 artificially aged samples (2 h, 6 h, 10 h)

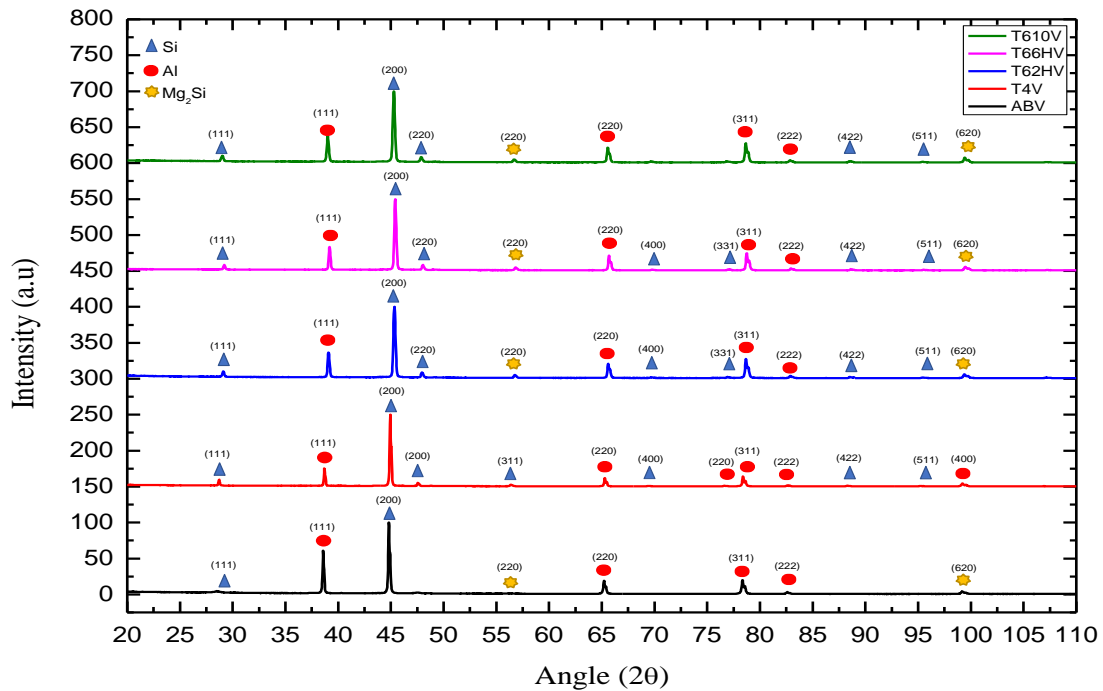


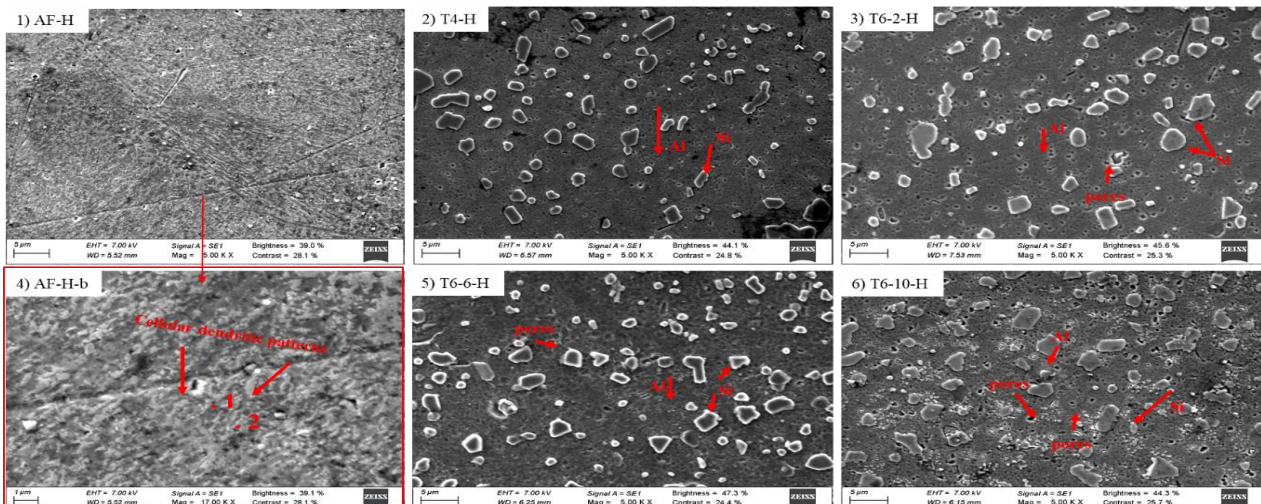
Figure 5c. XRD patterns of vertical (90°) AM-AISi10Mg samples AF-As fabricated, T4 naturally and T6 artificially aged samples (2h, 6h,10h)

3.3 Microstructural evaluation

The microstructure of samples was studied through a secondary electron method. The microstructure of AF samples consists of primary Al (dark region) within the majority of approximately 1 micron and Al-Si (lighter eutectic region), which can be seen in Figure 6. (AF-V-a; AF-V-b; AF-H-a; AF-H-b ; AF-T-a; AF-T-b) The eutectic structure located between some Al cells and enrichment of Si was also detected along the Al cell boundaries. The global microstructure of AM-AISi10Mg alloys after T4 (T4-V; T4-H ; T4-T) and 2 h, 6 h, 10 h, and SHT at 530°C is displayed in Fig. 6 (T6-2-V; T6-2-H; T6-2-T ; T6-6-V; T6-6-H; T6-6-T ; T6-10-V; T6-10-H; T6-10-T). Transformation of the microstructure by coarsening of Si particles during the SHT process was observed since columnar and "fish-scale" melt

pool features disappeared distinctively. The morphology and distribution of Si particles were further discovered in SEM micrographs in Figures. The predominance of Si particles seems to have an improper shape in all directions. The size variation lies approximately 500 nm to 5 µm while the aspect ratio remains similar in all directions.

In addition, no noticeable difference in shape and density of Si particles for Horizontal, Transverse, and Vertical cross-sections after the SHT were observed. Precipitate's approximate length was typically 1 – 5 µm and had a width of < 500 nm. EDS analysis performed to correctly recognise the precipitates. It is revealed that these precipitates were supplemented in iron (Fe). Moreover, coarsening and shape irregularity of Si particles are affected by T6 heat treatment time.



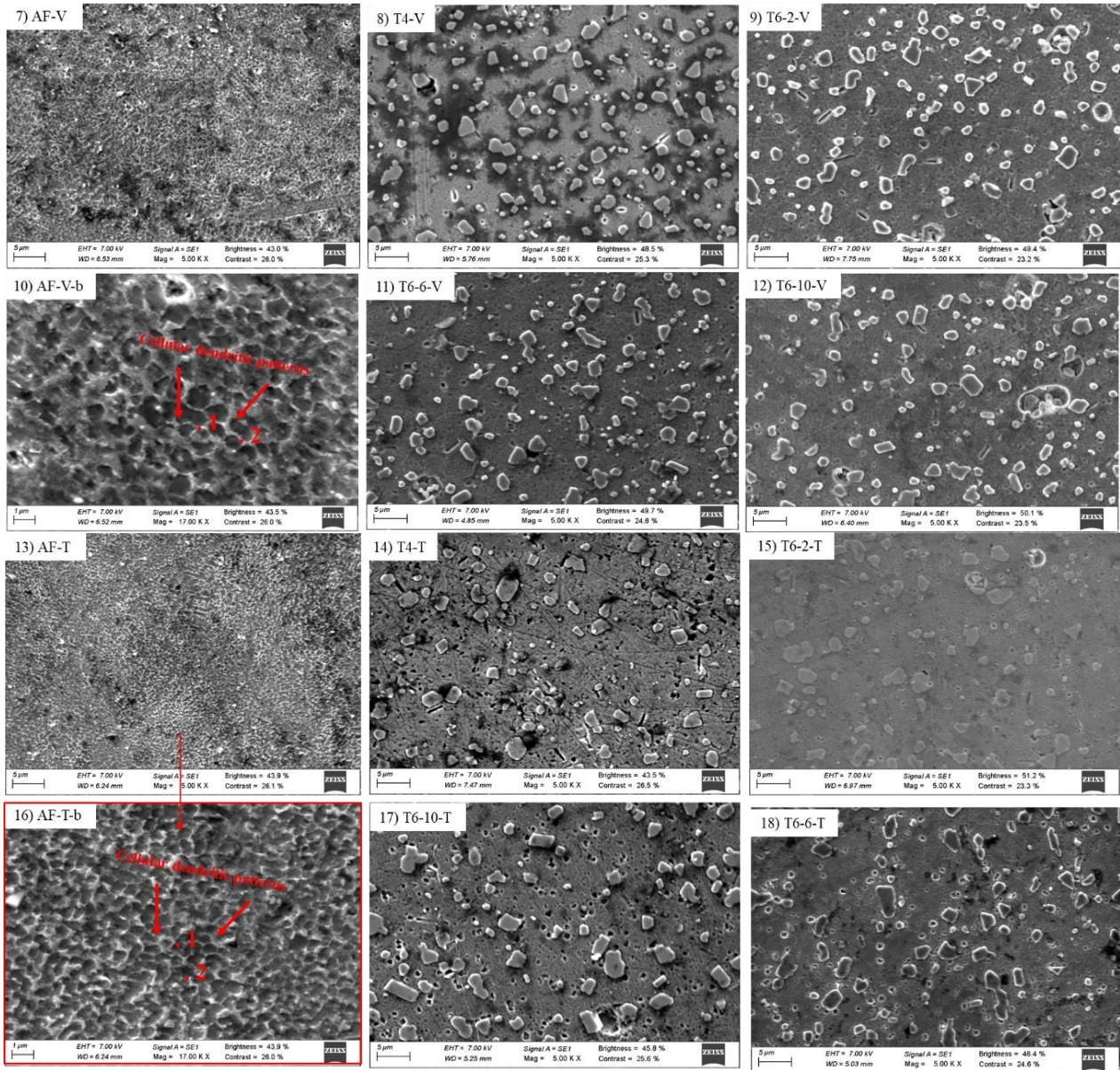


Figure 6. SEM view of samples. AF; As-Fabricated, T4; Natural Ageing; T6; Artificial Ageing. (H: Horizontal; V: Vertical; T: Transversal)

4 Conclusion

The effect of various post-process parameters was evaluated in this study for samples manufactured with different direction samples.

- This study paves the way for part manufacturers to identify specific post processes and choose the most suitable parameters for their design.
- The study may be further extended to evaluate the influences on mechanical properties of different heat treatments.
- Optimum heat treatment parameters regarding hardness are 2 hours at a time at 200 °C for all manufacturing directions.
- Especially in terms of time and cost for industrial applications, the method of obtaining parts with high

hardness and strength with direct heat treatment bypassing SHT needs to be investigated in detail.

Acknowledgement

This study is a part of the project (# 5189901) supported by The Scientific and Technological Research Council of Turkey (TÜBİTAK) under the Frontier R&D Laboratory Support Programme and hosted in Turkish Aerospace Industries Inc. The authors also acknowledge the support of King Fahd University of Petroleum and Minerals (KFUPM) in Saudi Arabia, Gazi University Turkey, and King Abdullah City for Atomic and Renewable Energy (K.A.CARE) to accomplish this work.

Conflict of interest

The authors declare that there is no conflict of interest.

Similarity index (iThenticate): %2

References

- [1] B. Saleh et al., 30 Years of functionally graded materials: An overview of manufacturing methods, Applications and Future Challenges, *Composite Part B Engineering*, 201, 108-376, 2020. <https://doi.org/10.1016/j.compositesb.2020.108376>.
- [2] J. Y. Lee, J. An, and C. K. Chua, Fundamentals and applications of 3D printing for novel materials, *Applied Materials Today*, 7, 120-133, 2017. <https://doi.org/10.1016/j.apmt.2017.02.004>.
- [3] Wohlers T, Campbell RL, Wohlers report 2020: 3D printing and additive manufacturing state of the industry annual worldwide progress report. Fort Collins, Colo: Wohlers Associates; 2020.
- [4] L. Yi, C. Gläßner, and J. C. Aurich, How to integrate additive manufacturing technologies into manufacturing systems successfully: A perspective from the commercial vehicle industry, *Journal of Manufacturing Systems*, 53, 195-211, 2019. <https://doi.org/10.1016/j.jmsy.2019.09.007>.
- [5] J. J. Lewandowski and M. Seifi, Metal additive manufacturing: A Review of mechanical properties, *Annual Review of Material Research*, 46, 151-186, 2016. <https://doi.org/10.1146/annurev-matsci-070115-032024>.
- [6] A. Majeed, Y. Zhang, J. Lv, T. Peng, Z. Atta, and A. Ahmed, Investigation of T4 and T6 heat treatment influences on relative density and porosity of AlSi10Mg alloy components manufactured by SLM, *Computational Industrial Engineering*, 139, 106-194, 2020. <https://doi.org/10.1016/j.cie.2019.106194>.
- [7] L. Zhou, A. Mehta, E. Schulz, B. McWilliams, K. Cho, and Y. Sohn, Microstructure, precipitates and hardness of selectively laser melted AlSi10Mg alloy before and after heat treatment, *Materials Characterization*, 143, 5-17, 2018. <https://doi.org/10.1016/j.matchar.2018.04.022>.
- [8] M. Moustafa, F. Samuel, H. Doty, Effect of solution heat treatment and additives on the microstructure of Al-Si (A413.1) automotive alloys, *Journal of Material Science*, 38, 4507-4522, 2003. <https://doi.org/10.1023/A:1027333602276>
- [9] I. Gutierrez-Urrutia, M. Munoz-Morris, D.G. Morris, Contribution of microstructural parameters to strengthening in an ultrafine-grained Al-7% Si alloy processed by severe deformation, *Acta Materials*, 55, 1319-1330, 2007. <https://doi.org/10.1016/j.actamat.2006.09.037>
- [10] B. Li, H. Wang, J. Jie, Z. Wei, Effects of yttrium and heat treatment on the micro-structure and tensile properties of Al-7.5 Si-0.5 Mg alloy, *Materials Design*, 32, 1617-1622, 2011. <https://doi.org/10.1016/j.matdes.2010.08.040>
- [11] M. Tang, P.C. Pistorius, J.L. Beuth, Prediction of lack-of-fusion porosity for powder bed fusion, *Additive Manufacturing*, 14, 39-48, 2017. <https://doi.org/10.1016/j.addma.2016.12.001>
- [12] NT. Aboulkhair, I. Maskery, C. Tuck, I. Ashcroft, N.M. Everitt, The microstructure and mechanical properties of selectively laser melted AlSi10Mg: The effect of a conventional T6-like heat treatment, *Material Science and Engineering*, 667, 139-146, 2016. <https://doi.org/10.1016/j.msea.2016.04.092>.
- [13] W. Li, S. Li, J. Liu, A. Zhang, Y. Zhou, Q. Wei, C. Yan, Y. Shi, Effect of heat treatment on AlSi10Mg alloy fabricated by selective laser melting: Microstructure evolution, mechanical properties and fracture mechanism, *Material Science and Engineering*, 663, 116-125, 2016. <https://doi.org/10.1016/j.msea.2016.03.088>.
- [14] L. Girelli, M. Tocci, M. Gelfi, A. Pola, Study of heat treatment parameters for additively manufactured AlSi10Mg in comparison with corresponding cast alloy, *Material Science and Engineering*, 739, 317-328, 2019. <https://doi.org/10.1016/j.msea.2018.10.026>.
- [15] K. Zygula, B. Nosek, H. Pasiowiec, N. Szysiak, Mechanical properties and microstructure of AlSi10Mg alloy obtained by casting and SLM technique, *Results in Materials* 104, 462-472, 2018.
- [16] X. Yu, L. Wang, T6 heat-treated AlSi10Mg alloys additively-manufactured by selective laser melting, *Procedia Manufacturing*, 15, 1701-1707, 2018. <https://doi.org/10.1016/j.promfg.2018.07.265>.
- [17] L. Zhou, A. Mehta, E. Schulz, B. McWilliams, K. Cho, Y. Sohn, Microstructure, precipitates and hardness of selectively laser melted AlSi10Mg alloy before and after heat treatment, *Material Characterisation*, 143, 5-17, 2018. <https://doi.org/10.1016/j.matchar.2018.04.022>.
- [18] E. Padovano, C. Badini, A. Pantarelli, F. Gili, and F. D'Aiuto, A comparative study of the effects of thermal treatments on AlSi10Mg produced by laser powder bed fusion, *Journal of Alloys Compound*, 831, 154-822, 2020. [doi: 10.1016/j.jallcom.2020.154822](https://doi.org/10.1016/j.jallcom.2020.154822).
- [19] A. Bendijk, R. Delhez, L. Katgerman, T.H. De Keijser, E.J. Mittemeijer, N.M. Van Der Pers, Characterization of Al-Si-alloys rapidly quenched from the melt, *Journal of Material Science*, 15, 2803-2810, 1980. <https://doi.org/10.1007/BF00550549>.
- [20] H.J. Axon, W. Hume-Rothery, The Lattice spacings of solid solutions of different elements in aluminium, *Proceedings of Royal Society London Series A Mathematical Physical and Engineering Science*, 193 1-24, 1948. <https://doi.org/10.1098/rspa.1948.0030>.
- [21] K.G.G. Prashanth, S. Scudino, H.J.J. Klauss, K.B.B. Surreddi, L. Löber, Z. Wang, a. K.K. Chaubey, U. Kühn, J. Eckert, Microstructure and mechanical properties of Al-12Si produced by selective laser melting: Effect of heat treatment, *Material Science and Engineering A*, 590, 153-160, 2014. <https://doi.org/10.1016/j.msea.2013.10.023>.
- [22] L. Hitzler, C. Janousch, J. Schanz, M. Merkel, B. Heine, F. Mack, W. Hall, A. Öchsner, Direction and location dependency of selective laser melted AlSi10Mg specimens, *Journal Materials Processing*

- and Technology, 243, 48–61, 2017. <https://doi.org/10.1016/j.jmatprotec.2016.11.029>.
- [23] J. Fite, S. Eswarappa Prameela, J. A. Slotwinski, and T. P. Weihs, Evolution of the microstructure and mechanical properties of additively manufactured AlSi10Mg during room temperature holds and low temperature aging, Additive Manufacturing, 36, 101-429, 2020. <https://doi.org/10.1016/j.addma.2020.101429>.
- [24] H. Ali, H. Ghadbeigi, K. Mumtaz, Effect of scanning strategies on residual stress and mechanical properties of selective laser melted Ti6Al4V, Material Science and Engineering A, 712, 175–187, 2018. <https://doi.org/10.1016/j.msea.2017.11.103>
- [25] H. Asgari, C. Baxter, K. Hosseinkhani, M. Mohammadi, On microstructure and mechanical properties of additively manufactured AlSi10Mg_200C using recycled powder, Material Science and Engineering A, 707, 148–158, 2017. <https://doi.org/10.1016/j.msea.2017.09.041>.
- [26] DD. Gu, W. Meiners, K. Wissenbach, R. Poprawe, Laser additive manufacturing of metallic components: materials, processes and mechanisms. International Materials Review, 57, 133–164, 2012. <https://doi.org/10.1179/1743280411Y.0000000014>
- [27] S. M. Yusuf, M. Hoegden, and N. Gao, Effect of sample orientation on the microstructure and microhardness of additively manufactured AlSi10Mg processed by high-pressure torsion, International Journal of Advance Manufacturing Technology, 106, 4321–4337, 2020. <https://doi.org/10.1007/s00170-019-04817-5>.
- [28] Z. H. Li, Y. F. Nie, B. Liu, Z. Kuai, M Zhao, and F.Liu, Mechanical properties of AlSi10Mg lattice structures fabricated by selective laser melting, Materials & Design, 192, 108-709, 2020.
- [29] A. Majeed, Y. Zhang, J. Lv, T. Peng, Z. Atta, and A Ahmed, Investigation of T4 and T6 heat treatment influences on relative density and porosity of AlSi10Mg alloy components manufactured by SLM, Computers & Industrial Engineering, 139, 106-194, 2020. <https://doi.org/10.1016/j.cie.2019.106194>
- [30] N. O. Larrosa, W. Wang, N. Read, M. Loretto, H. Evans, C. Carr, J. and, P. J. Withers, Linking microstructure and processing defects to mechanical properties of selectively laser melted AlSi10Mg alloy, Theoretical and Applied Fracture Mechanics, 98, 123-133, 2018. <https://doi.org/10.1016/j.tafmec.2018.09.011>

